JOURNAL OF MATERIALS SCIENCE 31 (1996) 589–602

Squeeze cast aluminium reinforced with mild steel inserts

G. DURRANT, M. GALLERNEAULT, B. CANTOR
Oxford Centre for Advanced Materials and Composites, Department of Materials, University of Oxford, Parks Road, Oxford OX1 3PH, UK

The bonding of a mild steel insert to an Al–7Si alloy during squeeze casting has been studied for a range of processing conditions. Assessment of the mild steel/Al–7Si alloy interface shear strength has been made with a push-out test, and the results have been correlated with microstructural observations and residual stress calculations. Uncoated inserts do not exhibit any significant reaction with Al–7Si because of rapid cooling of the melt during squeeze casting, giving a low interface shear strength of ~ 30 MPa. Preheating the inserts to 900 °C slightly improves the interface shear strength to ~ 45 MPa, but reaction between the steel and Al–7Si is prevented by the formation of an Fe_3O_4 magnetite layer on the steel surface. Inserts hot-dipped in molten Al–10Fe before squeeze casting have a much greater interface shear strength of ~ 110 MPa, with failure in the Al–7Si matrix rather than at the steel/Al–7Si interface. Inserts vacuum plasma spray coated with titanium have the greatest interface shear strength of ~ 130 MPa, without any interface reaction, because of mechanical keying of the rough splat-quenched titanium surface combined with high residual stresses in the Al–7Si matrix.

1. Introduction

There is considerable interest in replacing cast iron and steel automotive components such as brake discs, engine cylinder blocks and pistons with light weight aluminium castings to improve vehicle performance and efficiency [1]. The squeeze casting process, where solidification takes place under an applied pressure, has a number of benefits over conventional sand casting and permanent die methods [2–4]. The applied pressure provides excellent feeding of shrinkage porosity, such that the casting is virtually porosity free and risers are not required, and near net-shape components can be produced with good surface finish and dimensional control [2]. The high rate of heat extraction during solidification [3] allows relatively short casting times (~ 60 s), and results in a refined microstructure with good mechanical properties [4].

In structural components, the relatively low Young's modulus of aluminium alloys may present a problem and thus many studies have examined the prospect of reinforcing aluminium alloys with stiff ceramic fibres and particles, such as alumina and silicon carbide. The application of these composite materials has been limited, however, by their high cost and low fracture toughness (e.g. [5]). The use of a steel reinforcement offers a more cost-effective means of improving the mechanical properties of an aluminium alloy casting. However, mild steel and aluminium have a similar specific Young's modulus, and thus to reduce component weight the steel must be located in high load-bearing regions. For example, in components subject to a bending moment, the steel needs to be located away from the neutral axis in regions of high compressive and tensile stress. Other applications where a steel or cast iron insert may be of benefit include pistons with steel sealing ring grooves and engine cylinder blocks with wear-resistant steel liners [6].

One of the problems associated with steel inserts in an aluminium alloy casting is the necessity of forming a sound bond between the two metals [7]. When a cold insert is placed in the die, a poor bond results because of chilling of the molten aluminium around the insert together with surface oxide layers on the insert and casting alloy. To produce a good bond between ferrous metals and aluminium alloys, liquid metal hot-dipping processes have been developed [6, 8, 9] to wet the steel insert and coat it with a thin iron–aluminide reaction layer. The insert is then located in the die cavity and the aluminium alloy cast around it. This process results in a good metallurgical bond between the steel and aluminium, and has been applied to the production of aluminium alloy pistons with ferrous sealing ring grooves [6].

Despite the usefulness of bonding steel to aluminium alloys, little work has been published on the metallurgy of the interface or the mechanical properties of the bond. This paper describes an investigation into the integrity of the interface formed between mild steel inserts and a squeeze-cast Al–7 wt % Si alloy. To try and promote a good bond, hot-dipping was studied, as well as coating the steel with a reactive titanium layer. The interface shear strength was

0022–2461

investigated using a push-out test, and the results were correlated with microstructural observations and calculated residual stresses.

2. Experimental procedure

2.1. Insert preparation

Mild steel inserts were prepared from 6.35 mm diameter rod with the chemical composition given in Table I. The inserts were cut to a length of 70 mm, and a 2 mm diameter hole was drilled in one end. The inserts were bead blasted, immersed in nitric acid to remove surface deposits of iron hydroxide, washed with acetone, hot-dipped or titanium coated and finally located in the die cavity with a thermocouple in the 2 mm diameter hole.

Hot-dipping was carried out by immersing and gently stirring the inserts in a crucible of molten aluminium at 900 °C. Initial experiments indicated that saturating the aluminium melt with ~ 10 wt % Fe resulted in parabolic growth of an iron–aluminide reaction layer, without causing significant dissolution of the steel. The inserts were thus hot-dipped for 60 s, which provided complete wetting of the inserts with Al–10Fe and a final reaction layer thickness of ~ 140 μm.

Titanium coating of the inserts was effected by a vacuum plasma spraying (VPS) technique using a Plasmatechnik A2000 robot-controlled VPS system. Inserts were placed in the vacuum chamber, which was evacuated to 0.1 mbar and then back-filled with argon to ~ 150 mbar, and were then given a pre-coating sputter cleaning cycle, followed by plasma spraying with molten 99.6% pure titanium particles whilst the insert was rotated about its axis. After ten spraying passes, the insert was coated with titanium layer ~ 80 μm thick. The surface of the coating was relatively rough as a result of splat quenching of the molten titanium. To investigate the effect of this roughness on the interface shear strength, a number of inserts were ground on successively finer grades of SiC paper down to 1200 grit, to give a smoother surface finish.

2.2. Casting conditions

The squeeze-casting apparatus consisted of a 100 tonne hydraulic press with a cylindrical die and ram, as shown schematically in Fig. 1. This was used to produce castings 50 mm in diameter and 80 mm high. Thermocouples were located at the centre of the die cavity, towards the outside edge (at a radius of 17 mm) and in the die itself. A data logger was used to record temperature variations and the vertical displacement of the ram. To pre-heat the die prior to casting, the ram was lowered into the die cavity and a resistance furnace was placed around the die. In the majority of cases, the die cavity was lined with a 1 mm thick alumino-silicate insultating felt (Kaowool®) to reduce melt cooling prior to pressurization. This fibrous felt was infiltrated with molten Al–7Si during pressurization to give a good thermal contact between the melt and die.

TABLE I Composition of the mild steel inserts

C	Si	Mn	S	P
0.160	0.200	0.750	0.020	0.022

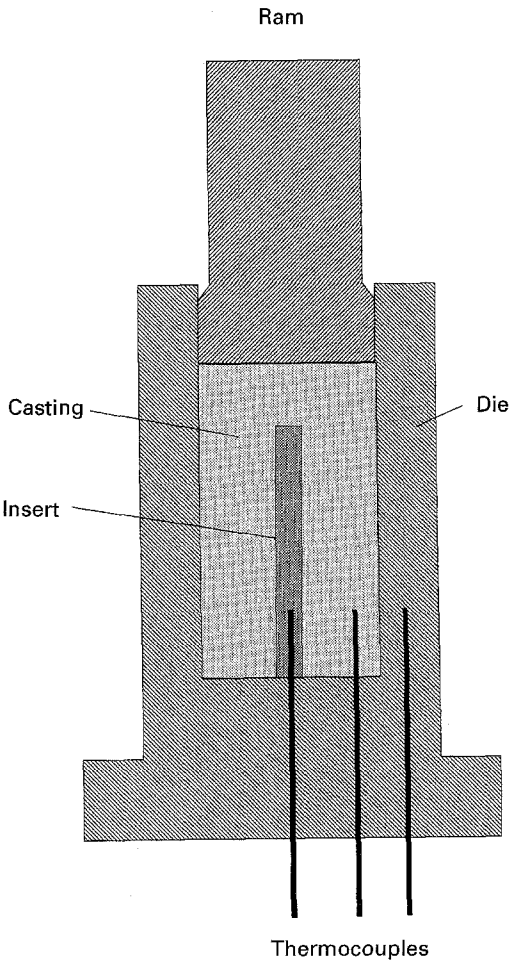

Figure 1 Schematic diagram of the squeeze-casting apparatus.

In a typical run, an insert was located on the centre thermocouple and the die, ram and insert assembly were pre-heated to 300 °C. Molten Al–7 wt % Si at 750 °C was then poured into the die cavity, and the ram was moved down into contact with the melt to apply a pressure of 100 MPa during solidification. The uncoated and titanium-coated inserts were pre-heated either to 300 °C in the die or to 900 °C in a furnace purged with argon. The inserts hot-dipped in molten Al–10Fe at 900 °C were placed quickly in the die cavity to minimize cooling prior to squeeze casting. The different insert coatings, pre-heat temperatures and die insulation conditions are given in Table II.

2.3. Interface shear strength

A push-out test was used to assess the mechanical integrity of the interface formed between the steel insert and the Al–7Si alloy. Five discs, ~ 7 mm thick, were machined from each casting, with care being taken to ensure that the insert remained parallel to the through thickness axis of the disc. The flat surfaces of the discs were then ground on SiC paper to remove machining damage.

TABLE II Insert coating conditions and number of castings

Coating technique	Nominal insert temperature (°C)	Insulating felt	Number of castings
Uncoated	300	No	1
Uncoated	900	Yes	2
Hot-dipped	900	Yes	2
Ti-coated	300	Yes	1
Ti-coated	900	Yes	1
Ti-coated and ground to 1200 grit	300	Yes	1
Ti-coated and ground to 1200 grit	900	Yes	1

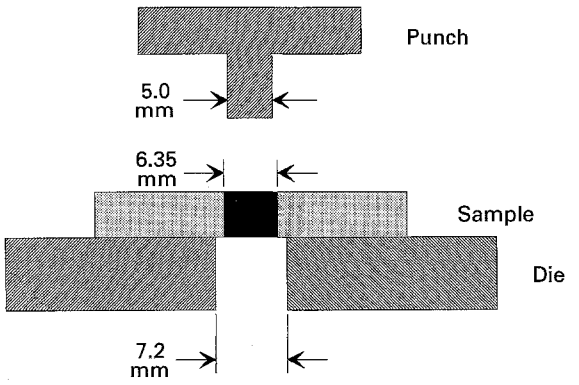

Figure 2 Schematic diagram of the push-out testing equipment.

The testing rig for the push-out tests is shown schematically in Fig. 2, and consisted of an H13 tool steel lower plate with a 7.2 mm diameter hole. A 7 mm thick disc from the casting was placed on the plate, and a 5.0 mm diameter H13 tool steel punch was used to push out the steel insert. The push-out tests were performed on an Instron 1195 testing machine, with the load on the punch and its displacement recorded continuously throughout the test. Shear stress values at the interface, τ, were established from the load, L and the surface area of the insert, using the following formula

$$\tau = L/[\pi D(t - d)] \quad (1)$$

where D is the diameter of the insert (6.35 mm), t is the specimen disc thickness, and d is the measured insert displacement, excluding elastic distortion.

2.4. Surface morphology and microstructural analysis

The surface roughness of the inserts prior to casting was investigated with a Philips 501 scanning electron microscope (SEM). The surface profile was measured using a Talysurf® profileometer, with a stylus radius of ~ 1 μm. Two roughness parameters were calculated from the surface profiles: (i) the surface height amplitude as the distance between the highest and lowest points over a sample length of 1 mm; and (ii) the centre line average (CLA) value as the arithmetic average of the profile above and below its mean height line over the sampling length [10].

Samples for microstructural analysis were taken from the top of each casting. These were mounted, ground on SiC paper, polished with successively finer grades of diamond slurry, and finally polished with colloidal silica. The identification of intermetallic and oxide phases was performed using a combination of energy dispersive spectroscopy (EDS) and wavelength dispersive spectroscopy (WDS) in a CAMECA SU30 microprobe.

3. Results

3.1. Uncoated inserts

SEM examination of the uncoated steel inserts revealed a pitted surface with no large deposits of iron hydroxide, as shown in Fig. 3a. Roughness traces such as that shown in Fig. 3b indicated that the surface height amplitude was 18.5 μm and the CLA value was 4.3 μm.

Fig. 4a shows typical cooling curves for the insert, melt and die thermocouples, together with corresponding measurements of ram travel during squeeze casting with an insert pre-heated to 300 °C. Initially

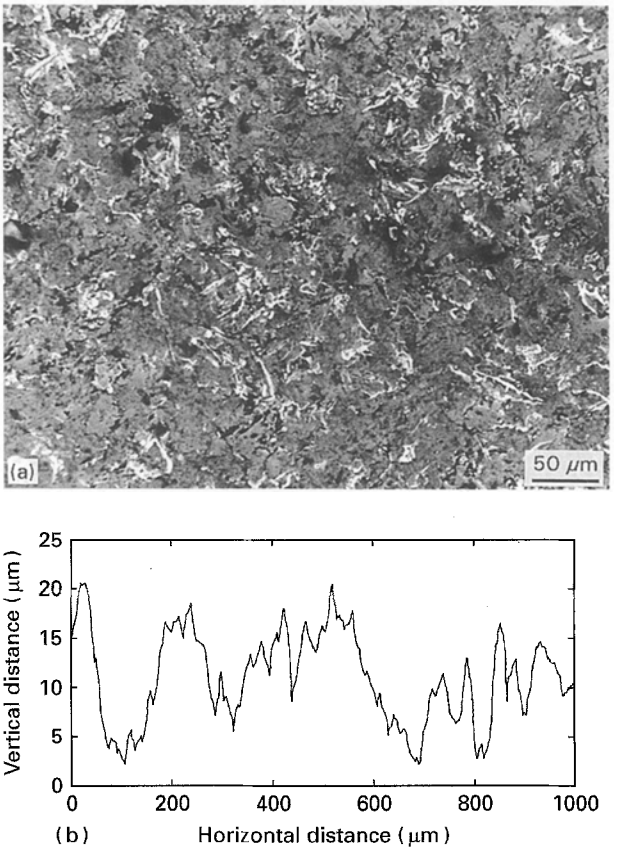

Figure 3 Surface of an uncoated insert; (a) scanning electron micrograph and (b) surface profile.

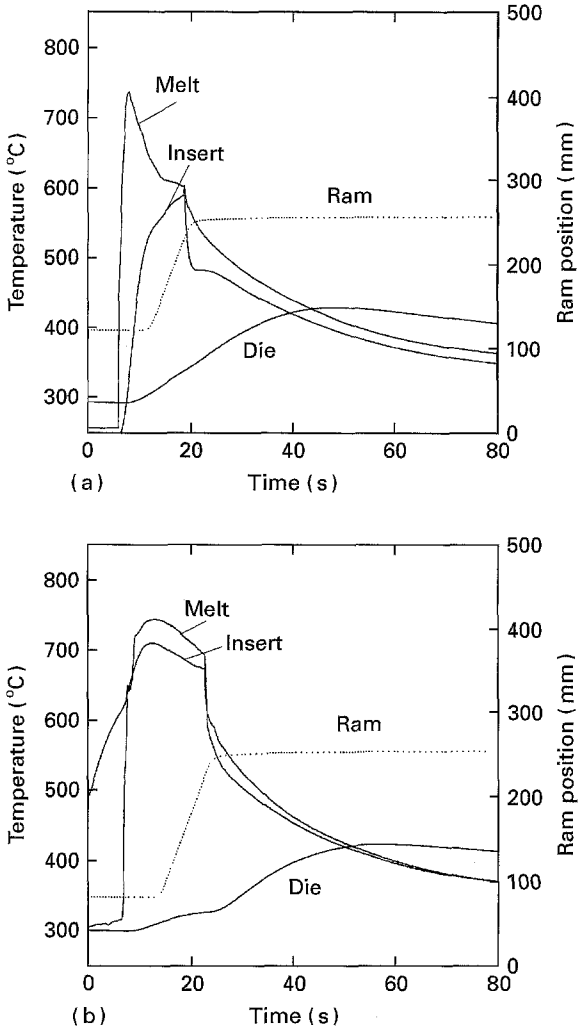

Figure 4 Cooling curves during squeeze casting with uncoated inserts pre-heated to (a) 300 °C and (b) 900 °C.

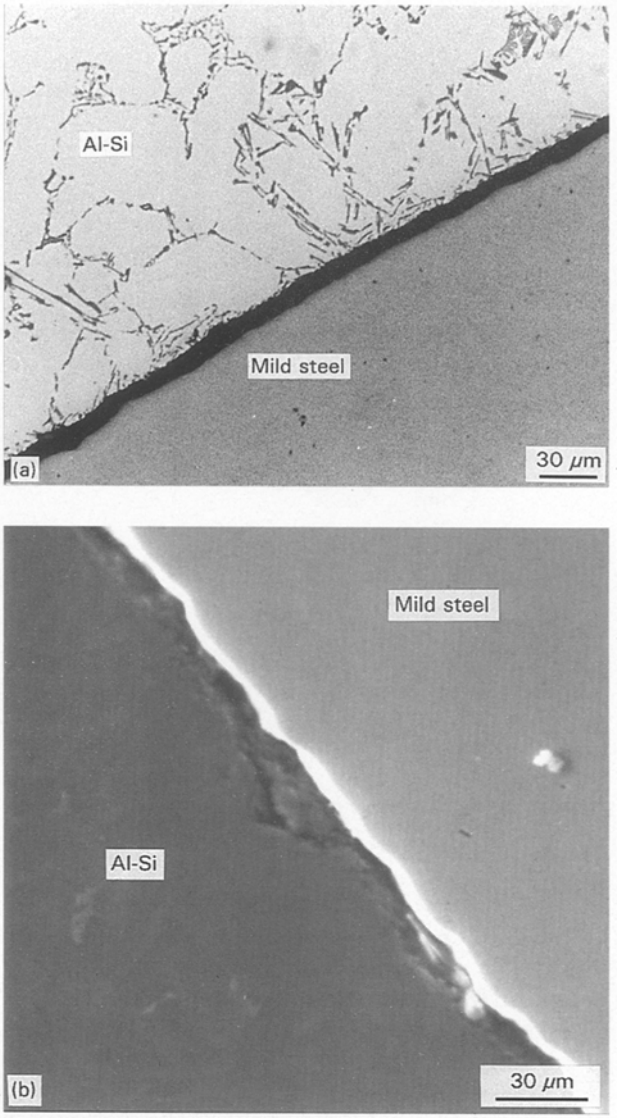

Figure 5 Uncoated inserts pre-heated to 300 °C; (a) optical micrograph and (b) scanning electron micrograph.

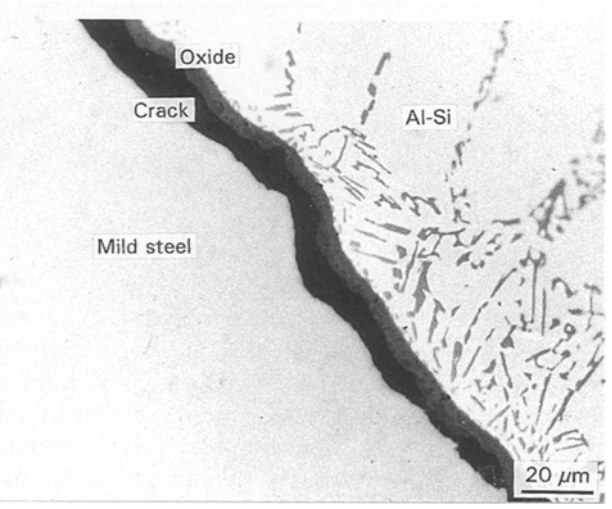

Figure 6 Optical micrograph of uncoated insert pre-heated to 900 °C.

the die temperature was ~ 300 °C, and after ~ 7 s, in Fig. 4a, the melt was poured into the die and the insert and melt temperatures increased to 600 °C and 730 °C, respectively. The melt then quickly cooled to 600 °C, ~ 15 °C below the liquidus temperature, as the ram moved down towards the molten metal. The ram reached the molten metal at ~ 18 s and pressurization commenced, causing a rapid drop in the melt and insert temperatures as a result of the greatly increased heat-transfer coefficient between the melt and die [3]. Solidification was complete after 22 s, in Fig. 4a, which was ~ 15 s after pouring of the melt.

Fig. 4b shows equivalent cooling curves for an insert pre-heated to 900 °C and a die lined with aluminosilicate insulating felt. The melt was poured into the die after ~ 7 s, at which time the die and insert temperatures were 300 and 650 °C, respectively. The insert and melt temperatures then increased to maximum values after ~ 13 s of 710 and 740 °C, respectively. The combination of insulating felt and pre-heating the insert to 900 °C resulted in much slower cooling, such that the melt temperature immediately before pressurization was 700 °C, compared with 600 °C for a die without insulation and an insert pre-heat of 300 °C, see Fig. 4a. After pressurization at ~ 22 s, there was a marked decrease in temperature as the insulating felt was infiltrated with molten Al–7Si to give a high heat-transfer coefficient. Solidification was complete after 25 s, which was ~ 18 s after pouring of the melt.

Fig. 5a and b show optical and scanning electron micrographs of the steel/Al–7Si interface for an

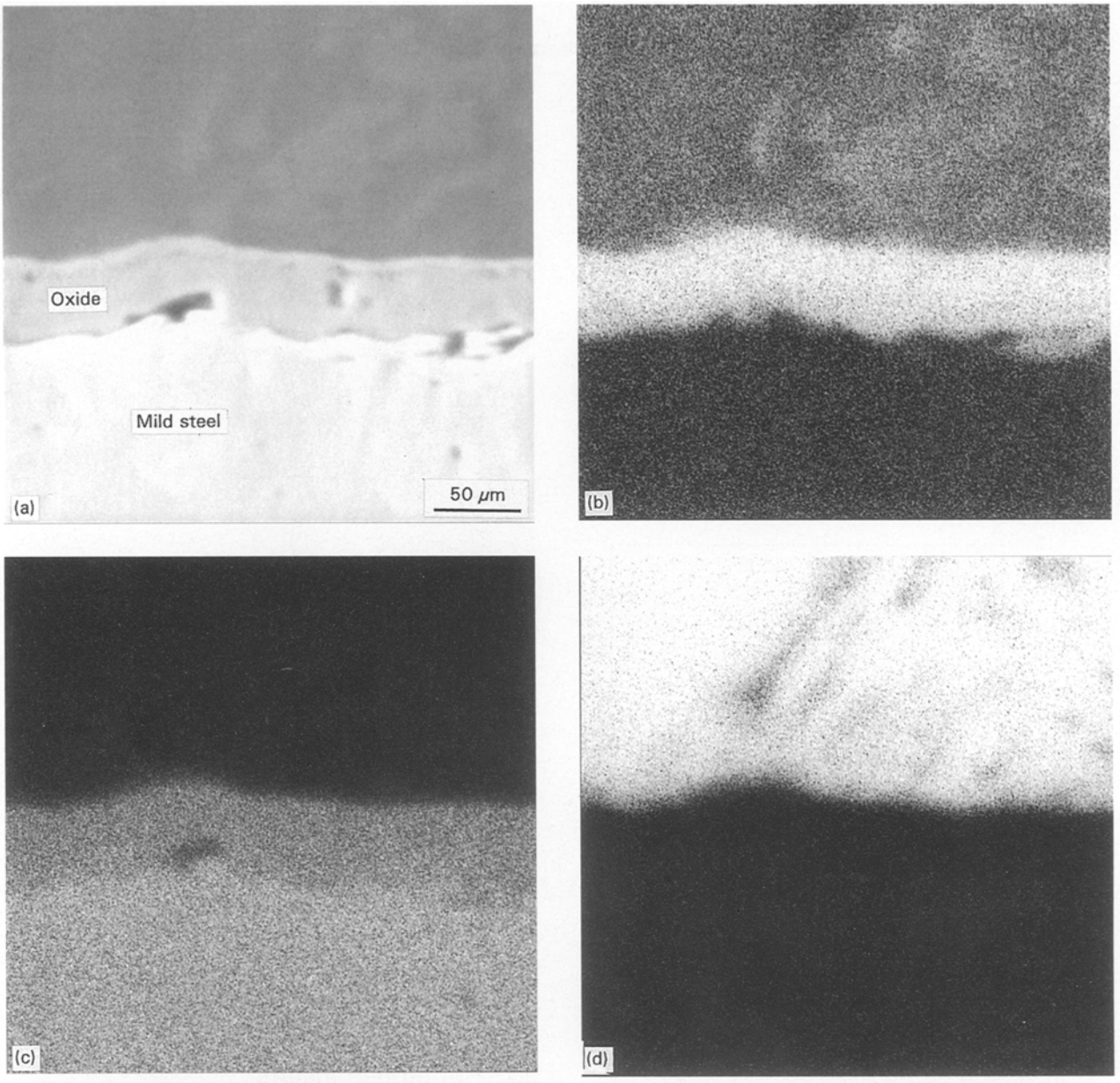

Figure 7 WDS concentration maps for an uncoated insert pre-heated to 900 °C; (a) scanning electron micrograph, (b) oxygen, (c) iron, (d) aluminium, and (e) silicon.

uncoated insert pre-heated to 300 °C. There was a crack 5–10 μm wide at the interface and little evidence any reaction between the two metals, and the matrix had a typical hypo-eutectic structure with no apparent porosity. Fig. 6 shows an optical micrograph of the steel/Al–7Si interface for an insert pre-heated to 900 °C. The interface was similarly cracked, with a dark layer ~ 5 μm thick adjacent to the Al–7Si matrix. Fig. 7 shows corresponding WDS concentration maps of the elements iron, oxygen, aluminium and silicon, which revealed that the dark layer was an iron oxide. Quantitative analysis gave an Fe/O atomic ratio of ~ 3/4, indicating stoichiometry of Fe_3O_4 magnetite.

Fig. 8a and b show push-out load–displacement curves in each case for a series of test specimens from one casting using an insert pre-heated to (a) 300 °C and (b) 900 °C. The number beside each curve in Fig. 8 corresponds to the position in the casting from which the test specimen was taken, numbering from the bottom upwards. For the 300 °C insert in Fig. 8a, the load increased sharply with displacement in a linear manner until the steel/Al–7Si interface failed at a load

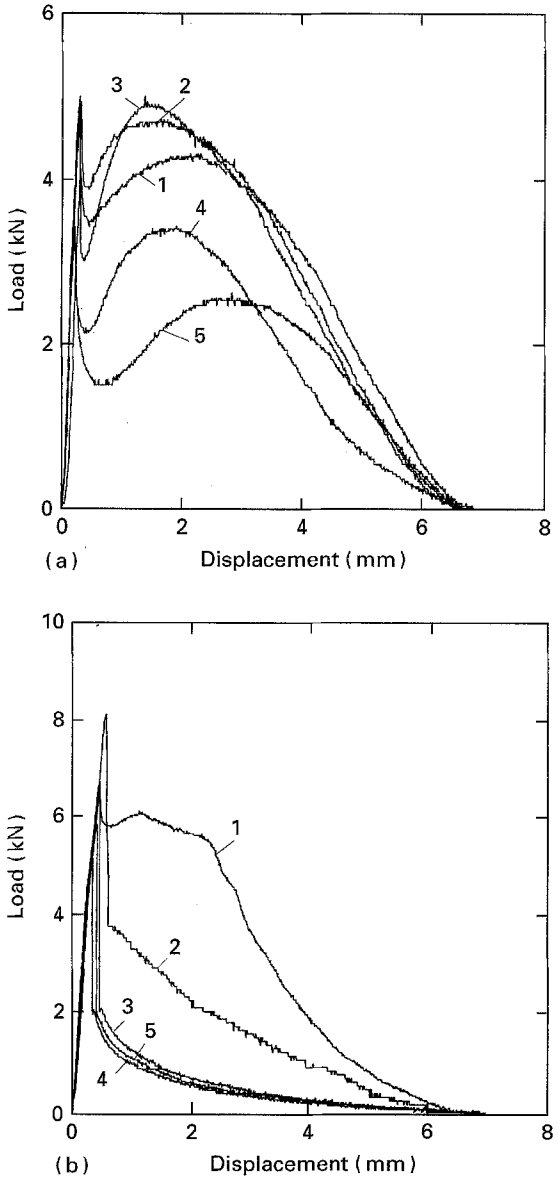

Figure 8 Push-out test results for uncoated inserts pre-heated to (a) 300 °C, and (b) 900 °C.

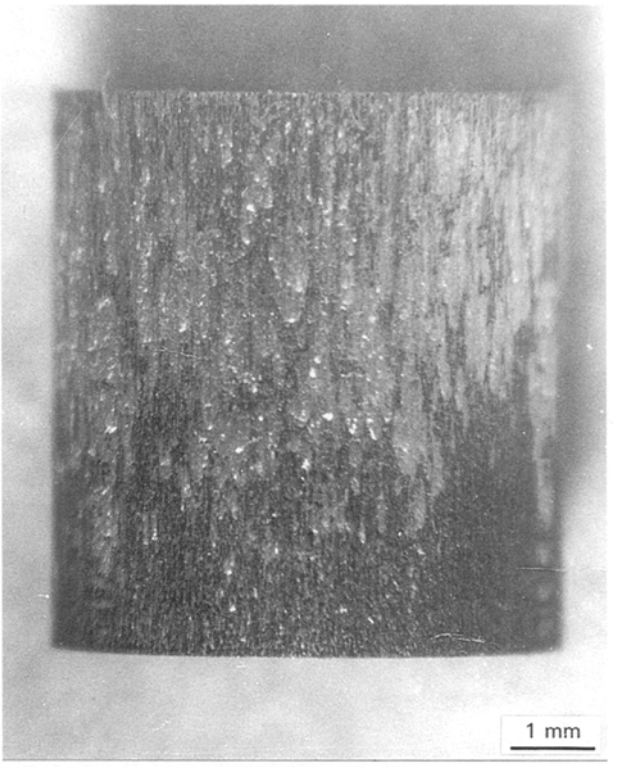

Figure 9 Uncoated insert after push-out testing.

TABLE III Interface shear strength, τ_i, for uncoated inserts

Insert temperature (°C)	Interface shear strength for each sample (MPa)					Mean strength (MPa)
	1	2	3	4	5	
300	30.3	36.1	36.2	25.1	25.1	30.5 ± 6.9
900	49.9	61.5	48.0	38.8	44.0	48.4 ± 10.5
900	44.5	37.4	44.0	39.7	36.8	40.5 ± 4.5

of 3–5 kN, with a subsequent load drop of 1–2 kN. This was followed by a gradual increase in load up to a maximum value, after which the load decreased as the insert was pushed out of the specimen disc, giving a final displacement value approximately equal to the specimen thickness. Examination of the inserts after testing, Fig. 9, revealed small patches of Al–7Si matrix smeared vertically along the surface. Heating the insert to 900 °C resulted in a greater interface failure load of 5–8 kN, as shown in Fig. 8b, although the load drop after failure was larger (2–4 kN) and there was no subsequent load increase. The extent of matrix adhesion on the pushed-out insert was less than for the insert heated to 300 °C.

Interface shear strengths, τ_i, were calculated from the push-out data in Fig. 8a and b at the point of interface failure using Equation 1, and the results are given in Table III. The mean interface shear strength of the inserts pre-heated to 900 °C was 44.5 MPa, somewhat greater than 30.5 MPa for the inserts pre-heated to 300 °C. There was no consistent trend in interface shear strength with specimen location.

3.2. Hot-dipped inserts

Fig. 10a shows a backscatter scanning electron micrograph of the insert surface after hot-dipping in Al–10Fe at 900 °C for 60 s. A reaction layer ~ 140 μm thick formed around the insert, and EDS analysis, Fig. 10b, revealed that it contained aluminium, iron and a trace of manganese. Quantitative WDS analysis identified this reaction layer as a mixture of iron aluminides, predominantly Fe_2Al_5 with some regions of $FeAl_3$. The iron aluminide grains appeared to have grown radially outwards from the steel surface, and contained ~ 10 vol % porosity. An outer aluminium-rich coating around the reaction layer was picked up during removal of the inserts from the reaction bath and this outer coating consisted of aluminium with ~ 16 vol % $FeAl_3$, i.e. corresponded to the hot-dipping bath composition (Al–10 wt % Fe).

Fig. 10c shows typical cooling curves during squeeze casting with hot-dipped inserts in a die lined with insulating felt. The cooling trends were similar to those observed during squeeze casting with uncoated inserts pre-heated to 900 °C (see Fig. 4b). When the melt was poured into the die after ~ 2 s, the die and insert temperatures were 300 and 650 °C, respectively, and the melt temperature immediately before

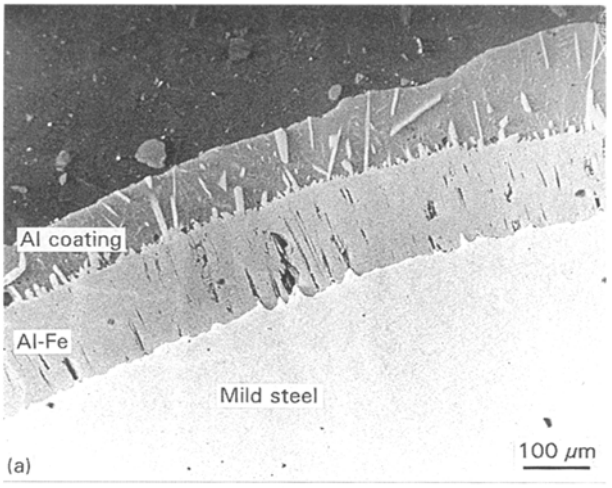

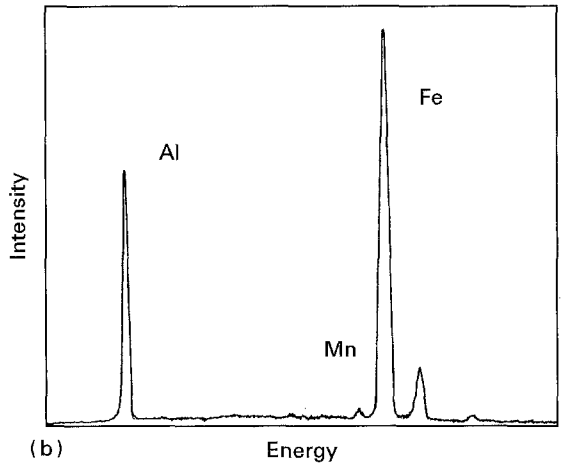

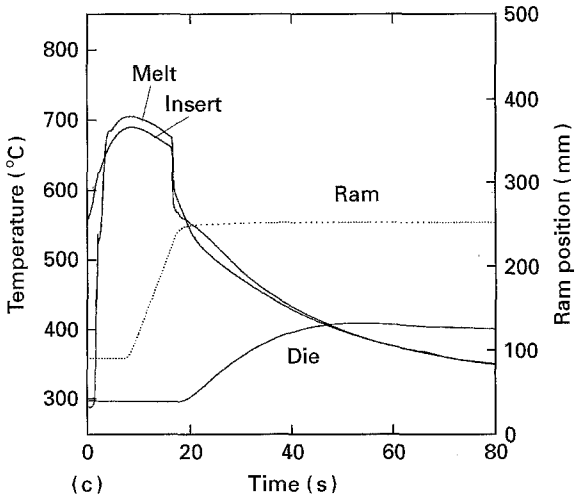

Figure 10 (a) SEM backscatter micrograph of a hot-dipped insert, (b) EDS trace of the iron-aluminide reaction phase, and (c) cooling curves during squeeze casting with a hot-dipped insert.

pressurization at ~ 17 s was 680 °C. Rapid cooling subsequent to pressurization resulted in a solidification time of ~ 18 s after pouring of the melt.

Fig. 11a and b show optical micrographs from two regions of the steel/Al–7Si interface after squeeze casting. The interface consisted of regions where an oxide film was present between the aluminium-rich outer coating on the hot-dipped insert and the Al–7Si matrix, Fig. 11a, and regions where the oxide was

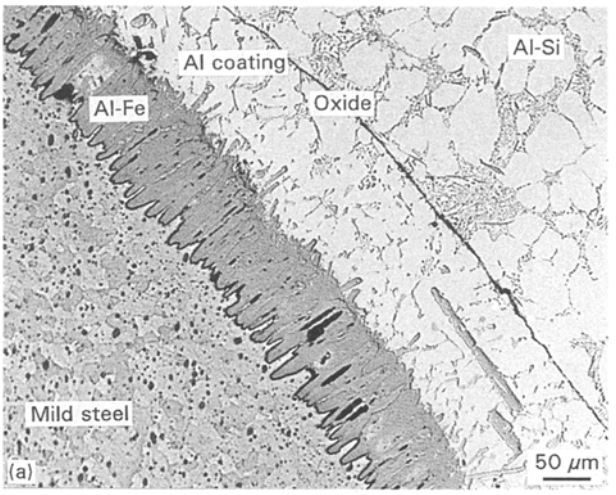

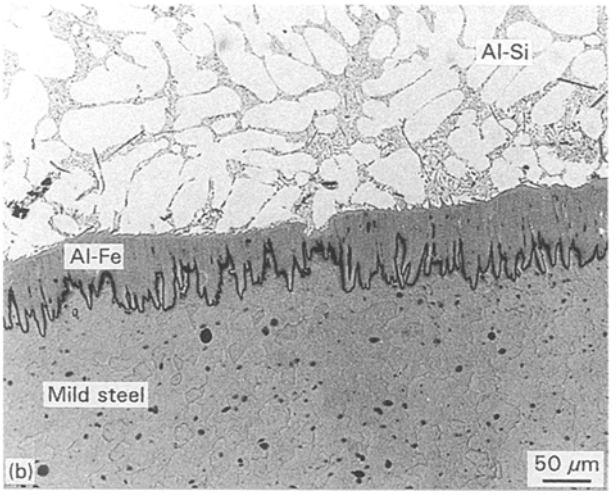

Figure 11 Optical micrographs of an Al–7Si squeeze casting with a hot-dipped insert showing (a) regions with an oxide layer, and (b) regions without an oxide layer.

removed leading to some dissolution of the aluminium-rich outer coating and the Fe_2Al_5 reaction layer, Fig. 11b. The oxide film was present on approximately 30% of the circumference of the insert.

Fig. 12a shows a series of push-out tests from one casting with a hot-dipped insert. The load required to force the insert out of the matrix was much greater for the hot-dipped inserts in Fig. 12a than for the uncoated inserts in Fig. 8 (note the change of scale). The initial linear region in Fig. 12a persisted up to a load of 12–16 kN, after which the load increased progressively more slowly towards a maximum value. This was followed by a decrease in load as the insert was pushed out of the sample, with a final displacement value approximately equal to the specimen thickness. After testing, the insert was found to be coated with an ~ 0.5 mm thick layer of Al–7Si, Fig. 12b, indicating that failure occurred in the matrix rather than at the steel/Al–7Si interface or at the oxide film shown in Fig. 11a.

Two interface parameters were calculated from the load–displacement curves for the hot-dipped inserts in Fig. 12a: (i) the interface yield strength, τ_y, at the end of the initial linear region; and (ii) the interface shear strength, τ_i, at the point of maximum load. These results are given in Table IV. The interface shear

strength was some 20 MPa greater than the interface yield strength. Furthermore, the mean interface shear strength of 113 MPa was much greater than the value of 45 MPa obtained for uncoated inserts pre-heated to 900 °C.

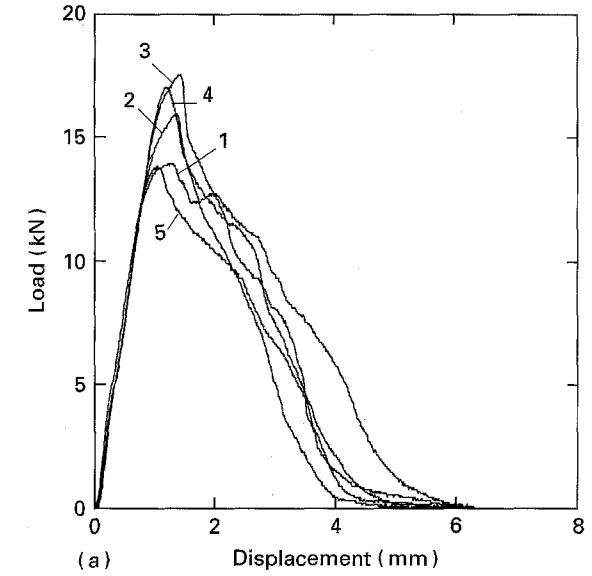

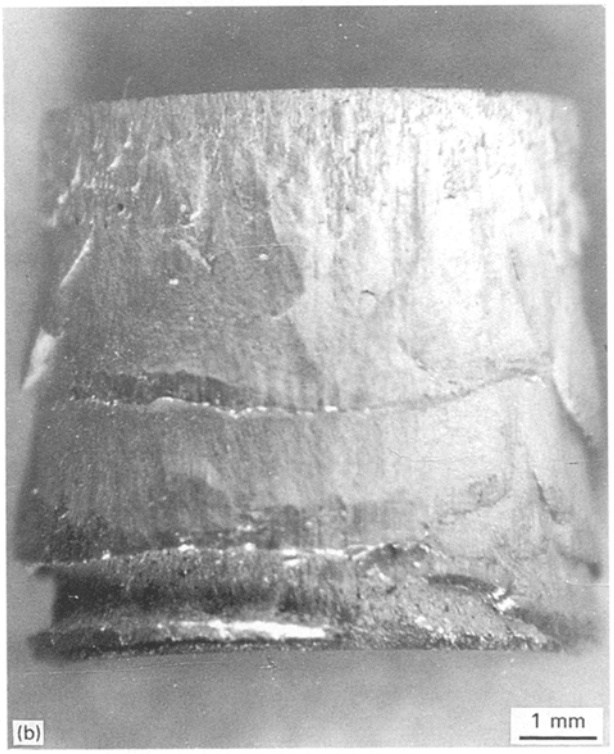

Figure 12 Hot-dipped inserts: (a) push-out test results, and (b) a typical insert surface after testing.

3.3. Titanium-coated inserts

Examination of the as-sprayed titanium-coated inserts revealed a rough, splat quenched surface, Fig. 13a. Talysurf® measurements, Fig. 13b, established that the surface height amplitude was 39 μm and the CLA value was 7.8 μm. After grinding on SiC paper down to 1200 grit, the surface height amplitude was reduced to less than 1 μm, as shown in Fig. 13c, and the CLA value correspondingly decreased to ~ 0.2 μm.

Fig. 14 shows cooling curves during squeeze casting with an insulated die and titanium-coated inserts

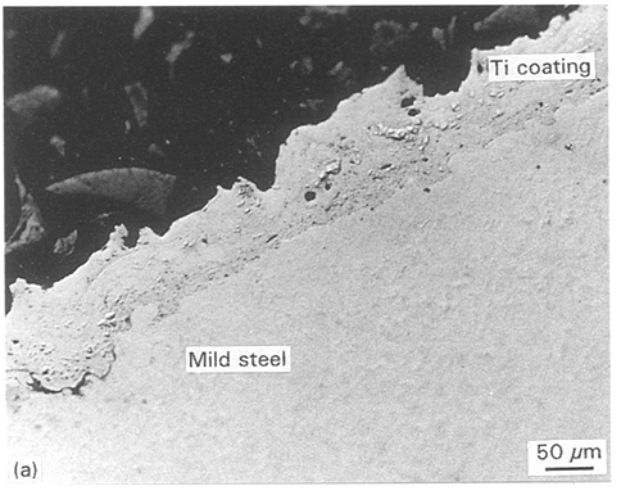

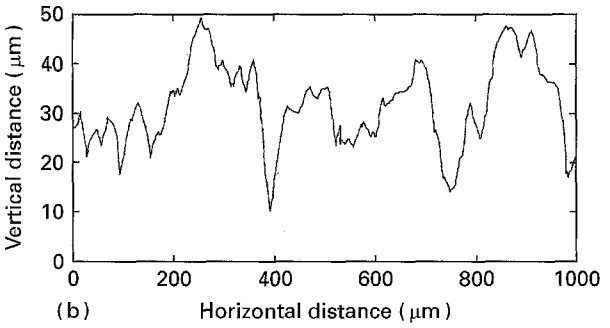

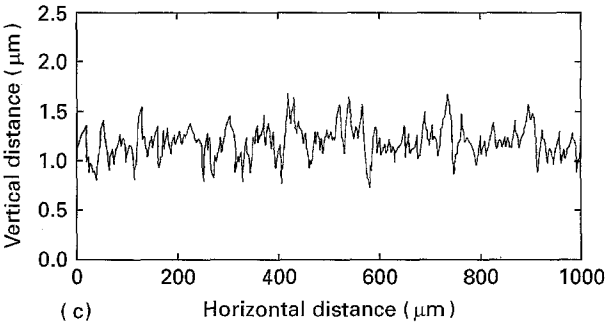

Figure 13 Titanium-coated inserts: (a) optical micrograph, (b) surface profile of as-sprayed insert, (c) surface profile after grinding.

TABLE IV Hot-dipped inserts; interface yield strength, τ_y, and interface shear strength, τ_i

Cast number	Interface yield strength for each sample (MPa)					Mean yield strength (MPa)	Interface shear strength for each sample (MPa)					Mean shear strength (MPa)
	1	2	3	4	5		1	2	3	4	5	
1	90.5	89.4	103	108	84.3	95.0 ± 12.4	101	116	128	125	100	114 ± 16.3
2	81.0	97.3	99.7	104	87.0	93.8 ± 11.8	92.7	121	117	124	105	112 ± 16.1

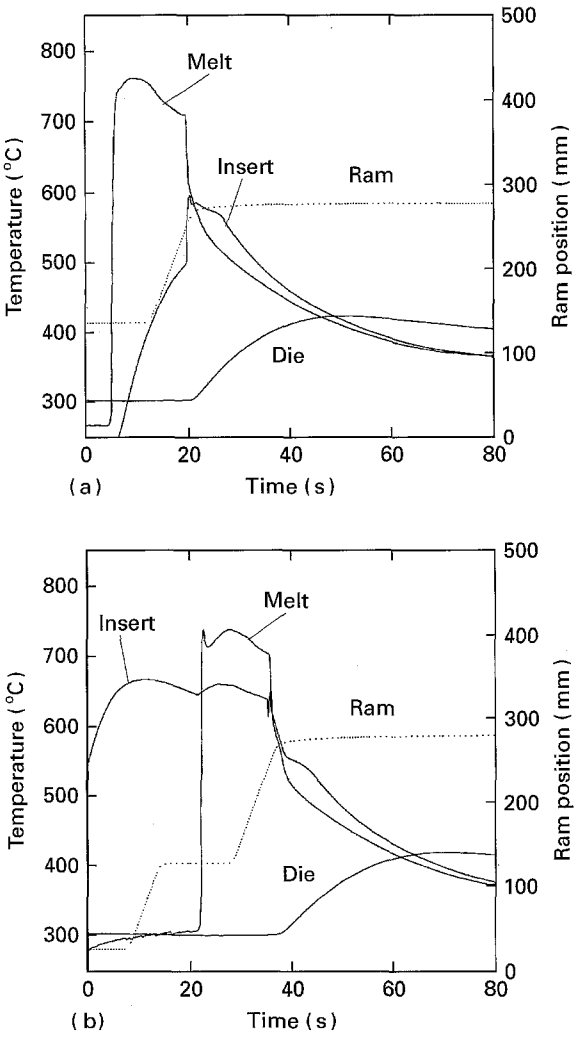

Figure 14 Cooling curves during squeeze casting with titanium-coated inserts pre-heated to (a) 300 °C, and (b) 900 °C.

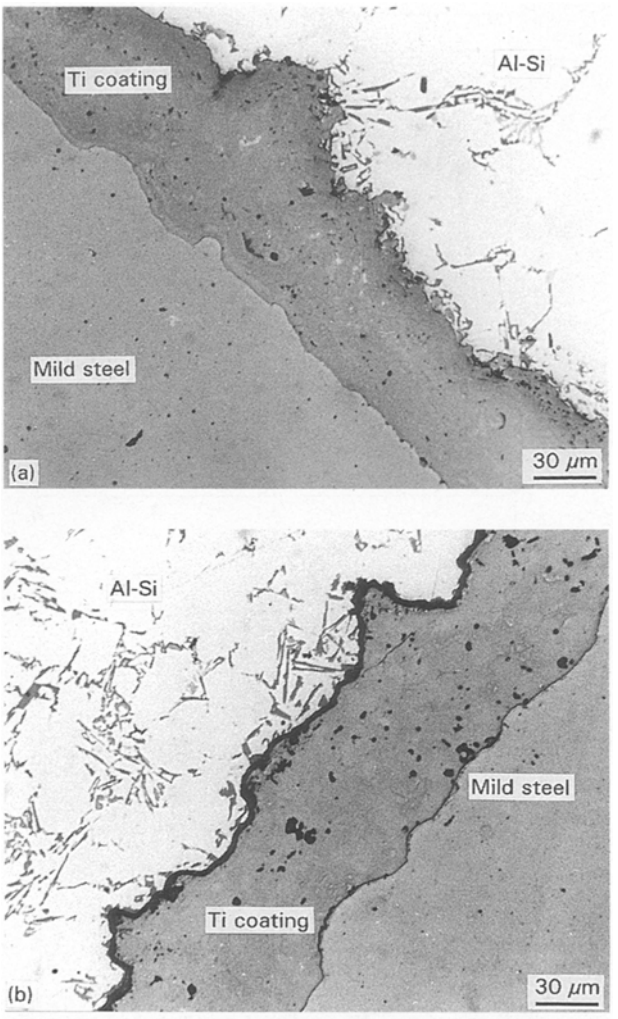

Figure 15 Optical micrographs of as-sprayed titanium-coated inserts pre-heated to (a) 300 °C, and (b) 900 °C.

pre-heated to (a) 300 °C and (b) 900 °C. For the insert pre-heated to 300 °C, the melt was poured into the die after ~ 5 s, and the insert and melt temperatures increased to 590 and 700 °C, respectively at the point of pressurization (~ 20 s). Solidification was complete after 22 s, i.e. ~ 17 s after pouring of the melt. For the insert pre-heated to 900 °C, the melt was poured into the die after ~ 22 s, and the insert and melt temperatures were 650 and 700 °C, respectively, at the point of pressurization (36 s). Solidification was complete ~ 20 s after pouring of the melt.

Fig. 15a shows an optical micrograph from a casting with an as-sprayed titanium coated insert pre-heated to 300 °C. No reaction between the titanium coating and the Al–7Si matrix was observed. However, the optical micrograph Fig. 15b for an insert pre-heated to 900 °C shows a dark layer ~ 4 μm thick between the titanium coating and the Al–7Si matrix. WDS analysis revealed that this layer contained the elements titanium, oxygen and aluminium with the approximate atomic ratio 28:61:11.

Fig. 16a and b show push-out results for the as-sprayed titanium-coated inserts pre-heated to 300 and 900 °C. The push-out curves exhibited a similar trend to the hot-dipped samples shown in Fig. 12a, with a linear region followed by an increase in load towards a maximum value. The surfaces of the pushed out inserts were again coated with an ~ 0.5 mm thick layer of Al–7Si. Interface yield strength, τ_y, and interface shear strengths, τ_i, are given in Table V. Both the interface yield strength and the interface shear strength were slightly greater for the inserts pre-heated to 300 °C ($\tau_y = 125$ MPa and $\tau_i = 150$ MPa) compared with the inserts pre-heated to 900 °C ($\tau_y = 110$ MPa and $\tau_i = 126$ MPa). The push-out curves shown in Fig. 16c and d for the ground titanium-coated inserts were similar to those obtained for the uncoated inserts in Fig. 8, with a linear increase in load up to a peak value followed by a decrease in load. The interface shear strengths, τ_i, were calculated at the end of the linear region and are given in Table V. Compared with the as-sprayed titanium-coated inserts, the interface shear strengths were markedly reduced, although the inserts pre-heated to 900 °C had a greater interface shear strength (34.4 MPa) than those heated to 300 °C (4.7 MPa).

4. Discussion

4.1. Interface microstructure

Incorporating uncoated mild steel inserts at 300 °C into an Al–7Si squeeze casting results in a cracked interface with little evidence of any reaction between the steel and Al–7Si, see Fig. 5. This lack of reaction is

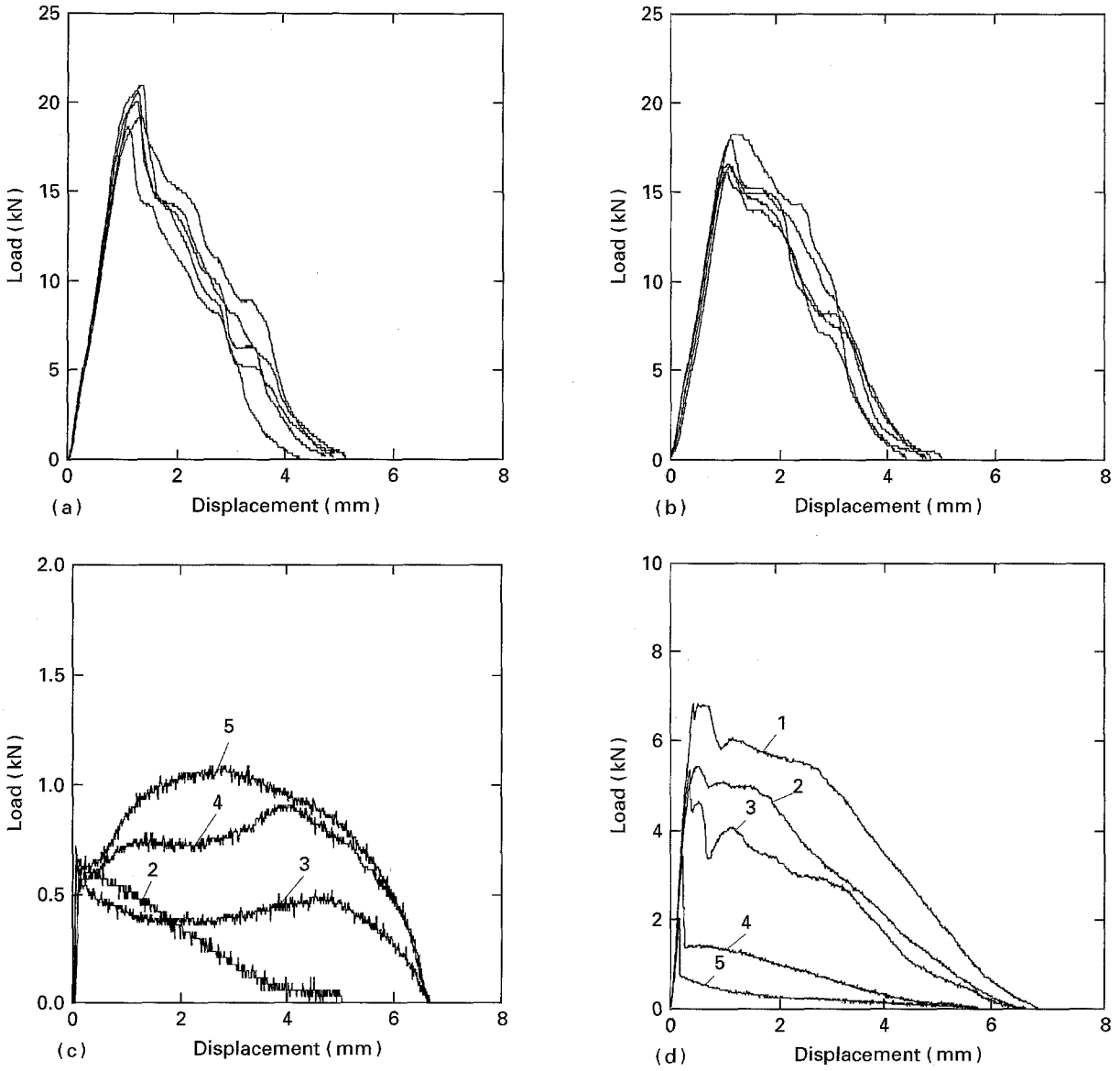

Figure 16 Push-out test results for titanium-coated inserts: (a) as-sprayed 300 °C, (b) as-sprayed 900 °C, (c) ground 300 °C, (d) ground 900 °C.

TABLE V Titanium-coated inserts: interface yield strength, τ_y, and interface shear strength, τ_i

Insert condition	Temperature (°C)	Interface yield strength for each sample (MPa)					Mean yield strength (MPa)	Interface shear strength for each sample (MPa)					Mean shear strength (MPa)
		1	2	3	4	5		1	2	3	4	5	
As-sprayed	300	121	128	126	124	124	125 ± 3.2	147	156	152	152	144	150 ± 5.8
	900	116	111	117	99.0	107	110 ± 9.1	135	123	132	119	123	126 ± 8.4
Ground	300							–	5.4	4.3	4.4	4.8	4.7 ± 0.7
	900							50.4	40.4	39.5	26.0	15.9	34.4 ± 16

due to rapid cooling of the molten Al–7Si around the relatively cool insert. The Fe–Al equilibrium phase diagram shows that the lowest temperature at which an iron aluminide phase is expected to form is 652 °C for $FeAl_3$ [11], and the cooling curves in Fig. 4a reveal that the melt temperature at a radius of 17 mm is above 652 °C for less than 5 s, and the reaction time available at the steel surface is even shorter as a result of melt quenching around the 300 °C insert. The crack at the interface forms when residual stresses are relaxed during sectioning of the casting for metallography, as discussed further in Section 4.2. There is still no reaction between the steel and the Al–7Si even when the inserts are pre-heated to the higher temperature of 900 °C, see Fig. 6. This is attributable to a 5 μm thick Fe_3O_4 magnetite layer on the steel surface, which probably forms when the insert is removed from the argon atmosphere of the pre-heat furnace and is located in the die cavity, a process which takes 10–15 s. The Fe_3O_4 layer is not reduced by the Al–7Si

melt, presumably because the Al–7Si alloy is liquid for less than 20 s during squeeze casting (see Fig. 4b).

Hot-dipping and stirring the inserts in molten Al–10Fe at 900 °C for 60 s results in full wetting of the insert and a reaction layer thickness of ~ 140 μm, see Fig. 10. The reaction layer is predominantly Fe_2Al_5, which accords with the findings of Yeremenko *et al.* [12], although some regions of $FeAl_3$ are also present. Other equilibrium iron-aluminium phases, which might be expected to form from the Fe–Al phase diagram, either do not nucleate or are consumed during the rapid growth of Fe_2Al_5 and $FeAl_3$. Removal of the insert from the hot-dipping bath results in an outer aluminium-rich coating on the insert surface, see Fig. 10a, and this coating oxidizes whilst the insert is located in the die cavity. During pouring of the Al–7Si melt, much of the oxide film is disrupted, although it remains intact on ~ 30% of the circumference of the insert (see Fig. 11).

Plasma-sprayed titanium coatings on inserts which are pre-heated to 300 °C and squeeze cast in an insulated die cavity do not react significantly with the Al–7Si melt, see Fig. 15a. This is because of rapid cooling during squeeze casting, with the Al–7Si being molten for less than 17 s, and quenching of the melt around the relatively cool insert. An additional barrier to the reaction of inserts pre-heated to the higher temperature of 900 °C is the formation of a 4 μm thick oxide layer on the titanium coating, although WDS analysis indicates that some reduction of this oxide does occur because the layer contains ~ 11 at % Al.

4.2. Mechanics of the push-out test

The mechanics of the push-out test have been studied for various fibre-reinforced ceramic matrix [13, 14] and metal matrix [15–17] composite materials. These studies have attempted to relate the load recorded in the push-out test to the interface shear strength. During the push-out test, the load first increases in a linear manner with punch displacement as the specimen deforms elastically. When the shear stress at the interface reaches a critical value, τ_i, the interface fractures and there is a decrease in load, after which the resistance to displacement is due to sliding friction, given by

$$\tau_{fr} = -\mu p \tag{2}$$

where μ is the coefficient of friction and p is the normal stress acting on the insert surface. The magnitude of p is determined by residual elastic stresses in the matrix, which are generated during cooling after squeeze casting in response to the difference in coefficient of thermal expansion, ΔCTE, between the matrix and the insert.

Residual stresses in a composite cylinder, see Fig. 17a, can be calculated as follows [18–21]. For an axisymmetric stress state, the principal stresses in polar co-ordinates are the radial stress, σ_r, the circumferential stress, σ_θ, and the axial stress, σ_z. Considering the stress equilibrium equations, the strain compatibility equations and the generalized thermoelastic stress–strain constitutive equations in polar co-ordinates, and further assuming that plane cross-sections of the

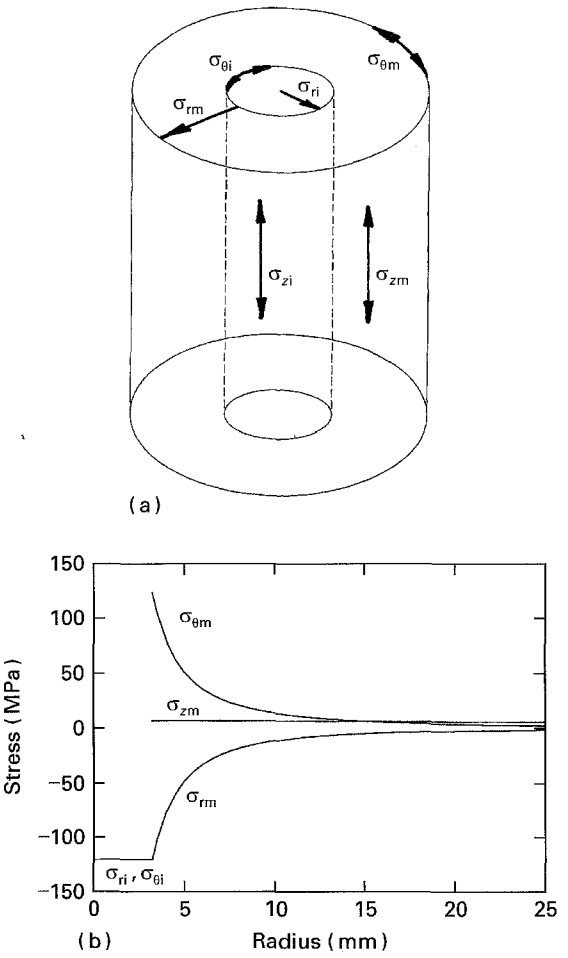

Figure 17 (a) Thick-walled composite cylinder model, and (b) calculated residual stresses in a squeeze casting containing a mild steel insert.

cylinder remain plane, it can be shown that the principal stresses are given by [18]

$$\sigma_{rs} = A_s - B_s/r^2 \tag{3a}$$

$$\sigma_{\theta s} = A_s + B_s/r^2 \tag{3b}$$

$$\sigma_{zs} = C_s \tag{3c}$$

where r is the radial distance from the cylinder axis, A and B are constants and the subscript s is replaced by i for the insert and m for the matrix (see Fig. 17a). For finite stress values at the centre of the insert, $B_i = 0$, such that [21]

$$\sigma_{ri} = \sigma_{\theta i} = A_i \tag{4}$$

The constants A_i, A_m, B_m, C_i and C_m can be established by imposing the following boundary conditions [19]: (i) no radial displacement at the main cylinder axis; (ii) displacement continuity at the insert/matrix interface; (iii) continuity of σ_r at the insert/matrix interface; (iv) $\sigma_r = 0$ at the matrix surface; (v) no net force over the ends of the cylinder. In terms of $\gamma = b/a$, where a and b are the radius of the insert and matrix respectively, the constants are [19]

$$A_m = \frac{E_i E_m \Delta\varepsilon}{D}[E_i(1 + \nu_m) + E_m(1 + \nu_i)(\gamma^2 - 1)] \tag{5a}$$

$$B_m = A_m b^2 \tag{5b}$$

$$C_m = \frac{E_i E_m \Delta\varepsilon}{D}[E_i(1+\nu_m)(\gamma^2+1) + E_m(1+\nu_i)(\gamma^2-1)] \quad (5c)$$

$$A_i = A_m(1-\gamma^2) \quad (5d)$$

$$B_i = 0 \quad (5e)$$

$$C_i = C_m(1-\gamma^2) \quad (5f)$$

where D is given by the determinant

$$\begin{vmatrix} 2[E_i\nu_m + E_m\nu_i(\gamma^2-1)] & E_i + E_m(\gamma^2-1) \\ E_i[1-\nu_m+\gamma^2(1+\nu_m)] + E_m(1-\nu_i)(\gamma^2-1) & E_i\nu_m + E_m\nu_i(\gamma^2-1) \end{vmatrix}$$

and E is Young's modulus, ν is Poisson's ratio and the term $\Delta\varepsilon$ is the misfit strain defined as

$$\Delta\varepsilon = (\alpha_m - \alpha_i)\Delta T \quad (6)$$

where α is the coefficient of thermal expansion (CTE) and ΔT is the net change in temperature as the casting cools. A value of $-200\,^\circ C$ has been used for ΔT, based on the assumption that the stresses generated in the initial stages of cooling are relieved by plastic relaxation of the Al–7Si matrix, until a temperature of 220 °C is reached [22, 23]. The thermoelastic properties of the mild steel insert and the Al–7Si matrix are given in Table VI [24].

In Fig. 17b the residual elastic stresses, calculated using Equations 3–6, are plotted as a function of radial distance (the axial stress in the insert, which is not shown, has a value of -450 MPa). Shrinkage of the Al–7Si around the insert results in a large radial compressive stress in the matrix, σ_m, with a value of -120 MPa at the insert surface, and this decreases in a parabolic manner towards the surface of the casting. The radial stress at the interface acts normal to the insert surface, and thus the value of p in the sliding friction Equation (2) may be taken as -120 MPa. In the axial direction, the matrix is in tension (7.4 MPa) and the insert in compression (-450 MPa). The large difference between these values is primarily due to the much greater cross-sectional area of the Al–7Si matrix compared with the insert. Furthermore, the insert is under a large compressive hydrostatic stress (-230 MPa), such that the high axial stress in the insert (-450 MPa) does not cause it to yield.

The above calculations of residual stress are based on a composite cylinder with a relatively large length to diameter ratio. Removal of the 7 mm thick discs for push-out tests will, however, significantly alter the residual axial stress state (σ_{zi}, σ_{zm}) because free surfaces are introduced perpendicular to the main cylinder axis. These free surfaces allow the insert, which is in axial compression, to expand and the Al–7Si matrix, which is in axial tension, to contract, thereby creating a shear stress at the steel/Al–7Si interface. The extent to which the axial stresses are relaxed depends on the interface shear strength, and the resultant axial stress distribution will be non-uniform along the length of the insert [25]. The crack observed at the steel/Al–7Si interface for uncoated inserts (see Fig. 5) is thus attributable to the relaxation of axial stresses during removal of the sample for metallography, and to an inherently low interface shear strength. Residual stresses in the radial and circumferential directions are not relaxed to such an extent when samples are removed from the casting because no free surfaces are created normal to these stress directions.

TABLE VI Material property data used in the residual stress calculations [24]

Property	Mild Steel	Aluminium
Young's modulus (GPa)	195	70
Poisson's ratio	0.30	0.33
Coefficient of thermal expansion ($10^{-6}\,^\circ C^{-1}$)	12.8	23.0

4.3. Interface shear strength

The push-out curves for uncoated inserts pre-heated to 300 °C (see Fig. 8) are characterized by a peak load followed by a load drop. The peak load is related to the interface shear strength, with a mean value of 30.5 MPa, and the load drop is caused by propagation of the crack along the length of the interface, see Fig. 5. After debonding, there is an increase in push-out load which is attributable to asperities on the insert, which have a surface height amplitude of ~ 20 μm, causing local deformation and work hardening of the surrounding matrix, as evidenced by the small patches of Al–7Si identified on the insert surface after testing (see Fig. 9). The coefficient of friction, calculated using Equation (2) and a normal stress of -120 MPa, thus increases from a value of ~ 0.17 immediately after debonding to a peak value of ~ 0.24. Pre-heating the inserts to 900 °C increases the interface shear strength to a mean value of ~ 44 MPa, although the subsequent load drop is greater, to a value which corresponds to a coefficient of friction of ~ 0.19, similar to that for inserts pre-heated to 300 °C. There is no load increase after debonding, and little Al–7Si matrix is visible on the insert surface after testing, indicating that failure occurs at the steel/Fe_3O_4 interface rather than at the Fe_3O_4/Al–7Si interface. Such an argument accords with the cracks observed between the steel and the Fe_3O_4 magnetite layer (see Fig. 6).

With hot-dipped inserts, the load–displacement curves in the push-out test (see Fig. 12) are significantly different from those exhibited by the uncoated inserts. Following a linear elastic region, the matrix yields and work hardens towards a maximum load value, without the subsequent load drop associated with debonding. The interface yield strength (94.4 MPa) and the interface shear strength (113 MPa) are much greater than the interface shear strength of uncoated inserts (30–44 MPa). Furthermore, a thick Al–7Si coating, with an outside radius similar to that of the hole in the lower die of the push-out rig, is present on the inserts following testing. These results show that failure occurs in the Al–7Si matrix, with fracture occuring at the diameter of the hole in the push-out rig. The maximum shear stress is, indeed, approximately what might be expected for a squeeze-cast Al–7Si alloy. For example, Chadwick and Yue [4] obtained a UTS value of 214 MPa for as-cast

LM25 alloy (Al–7Si–0.3Mg), which from von Mises yield criterion gives a shear strength of ~ 120 MPa. The concept of a coefficient of friction does not apply to the hot-dipped inserts because failure occurs in the matrix rather than at the steel/Al–7Si interface; indeed, the calculated value of μ corresponding to the interface shear strength is ~ 0.94, which is greater than the maximum value of 0.577 expected for full bonding at the interface with sub-surface shearing [26].

The effect of surface roughness on the interface shear strength is clearly demonstrated by the plasma-sprayed titanium-coated inserts. With inserts in the as-sprayed condition pre-heated to 300 °C, the push-out curves (see Fig. 16a) are similar to the hot-dipped inserts, with an interface shear strength of 150 MPa and failure in the matrix rather than at the steel/Al–7Si interface. However, grinding the titanium coating with SiC paper to 1200 grit reduces the surface height amplitude from ~ 40 μm in the as-sprayed condition to ~ 1 μm, and the interface shear strength correspondingly decreases to ~ 5 MPa, with a coefficient of friction of ~ 0.04. These results show that the bond between titanium coated inserts and the Al–7Si matrix is weak, but large surface height amplitude (~ 40 μm) combined with a high residual radial stress (– 120 MPa) can still lead to a large interface shear strength and failure in the Al–7Si matrix. The effect of surface roughness on sliding friction is further evidenced by the ground titanium-coated inserts. A surface height amplitude of ~ 1 μm gives a coefficient of friction of ~ 0.04, considerably lower than ~ 0.20 for the uncoated inserts, which have a surface height amplitude of ~ 20 μm. The theoretical treatments of Jero *et al.* [14] and Mackin *et al.* [17] have considered surface roughness effects by calculating the separate contributions to p in Equation (2) arising from the residual radial stress and the additional normal stress arising from surface asperities at the interface. Such an analysis is inappropriate in the present case, because the Al–7Si matrix is relatively soft, and thus matrix asperities deform plastically rather than slide over asperities on the insert surface. Pre-heating the ground titanium-coated inserts to 900 °C results in a larger coefficient of friction of ~ 0.20, larger than inserts pre-heated to 300 °C, and this is related to the limited reaction between the oxide layer on the titanium coating and the Al–7Si matrix during squeeze casting.

5. Conclusion

Squeeze casting Al–7Si with a mild steel insert at 300 °C does not result in any significant reaction at the interface, because of rapid cooling of the melt around the relatively cool insert. Push-out tests reveal a relatively low interface shear strength of ~ 30 MPa. Pre-heating the inserts to 900 °C does not significantly improve the interface shear strength (~ 45 MPa) because reaction between the steel and Al–7Si is prevented by the formation of the Fe_3O_4 magnetite layer on the steel surface.

However, squeeze casting Al–7Si with a mild steel insert hot-dipped in Al–10Fe at 900 °C for 60 s greatly improves the interface shear strength to ~ 110 MPa, with failure in the Al–7Si matrix rather than at the steel/Al–7Si interface. This increase in the interface shear strength is due to wetting of the insert with Al–10Fe prior to squeeze casting and to the formation of an iron aluminide reaction layer on the steel surface.

Squeeze casting Al–7Si with a mild steel insert vacuum plasma-spray coated with titanium does not result in significant reaction at the interface, even when the insert is pre-heated to 900 °C. However, in the rough as-sprayed condition the interface shear strength is 150 MPa, because of a large surface height amplitude (~ 40 μm) combined with high residual radial stresses in the Al–7Si matrix (~ 120 MPa). After grinding the titanium-coated inserts to reduce the surface height amplitude to ~ 1 μm, the interface shear strength is correspondingly decreased to ~ 5 MPa.

Acknowledgements

We thank Mr C. Salter for assistance with the WDS analysis and Drs J. Durodola, P. R. G. Anderson and B. Derby for helpful discussions. The research was funded by the SERC, DTI, Cookson Precision Castings and Lucas Automotive. One of us (MG) acknowledges NATO/NSERC (Canada) for provision of a science fellowship.

References

1. T. W. CLYNE and P. J. WITHERS, "An introduction to Metal Matrix Composites" (Cambridge University Press, Cambridge, 1993).
2. J. R. FRANKLIN and A. A. DAS, *Br. Foundry.* **77** (1984) 150.
3. J. A. SEKHAR, G. J. ABBASCHIAN and R. MEHRABIAN, *Mater. Sci. Eng.* **40** (1979) 105.
4. G. A. CHADWICK and T. M. YUE, *Metals Mater.* **5** (1989) 6.
5. P. M. MUMMERY and B. DERBY, in "Proceedings of the 12th Risø International Symposium on Materials Science", Roskilde, Denmark, September 1991, edited by N. Hansen, D. Juul Jensen, T. Leffers, H. Lilholt, T. Lorentzen, A. S. Pedersen O. B. Pedersen and B. Ralph, p. 535.
6. L. SULPRIZIO, "Manufacture of Pistons", US Pat. 2620530, 9 December 1952.
7. H. G. KANG, D. L. ZHANG and B. CANTOR, *J. Microsc.* **169** (1993) 239.
8. M. G. WHITFIELD and V. SHESHUNOFF, "Coating Metals", US Pat. 2396730, 19 March 1946.
9. *Idem*, "Aluminium Coating Process", US Pat. 2453772, 16 November 1948.
10. A. J. T. SCARR, "Metrology and Precision Engineering" (McGraw-Hill, London, 1967).
11. T. B. MASSALSKI, "Binary Alloy Phase Diagrams", 2nd Edn (ASM International, Metals Park, OH, 1990).
12. V. N. YEREMENKO, V. NATANZON and V. I. DYBKOV, *J. Mater. Sci.* **16** (1981) 1748.
13. R. J. KERANS and T. A. PARTHASARATHY, *J. Am. Ceram. Soc.* **74** (1991) 1585.
14. P. D. JERO, R. J. KERANS and T. A. PARTHASARATHY, *ibid.* **74** (1991) 2793.
15. T. W. CLYNE and M. C. WATSON, *Compos. Sci. Technol.* **42** (1991) 25.
16. P. D. WARREN, T. J. MACKIN and A. G. EVANS, *Acta Metall. Mater.* **40** (1992) 1243.
17. T. J. MACKIN, P. D. WARREN and A. G. EVANS, *ibid.* **40** (1992) 1251.
18. S. P. TIMOSHENKO and J. N. GOODIER, "Theory of Elasticity", 3rd Edn (McGraw-Hill, New York, USA, 1970).

19. G. W. SCHERER, "Relaxation in Glass and Composites" (Wiley, London, 1986).
20. H. PORITSKY, *Physics* **5** (1934) 406.
21. K. BRUGGER, *Appl. Opt.* **10** (1971) 437.
22. R. J. ARSENAULT and M. TAYA, *Acta Metall.* **35** (1987) 651.
23. M. VOGELSANG, R. J. ARSENAULT and R. M. FISHER, *Metall. Trans.* **17A** (1986) 379.
24. "Metals Handbook", 9th Edn (ASM International, Metals Park, OH, 1978).
25. G. D. REDSTON and J. E. STANWORTH, *J. Soc. Glass Technol.* **30** (1946) 201.
26. G. E. DIETER, "Mechanical Metallurgy", 3rd Edn (McGraw-Hill, London, 1988).

Received 11 January
and accepted 15 August 1995